IEEE Access
Multidisciplinary ⋮ Rapid Review ⋮ Open Access Journal

Received January 12, 2021, accepted February 12, 2021, date of publication February 16, 2021, date of current version February 24, 2021.

Digital Object Identifier 10.1109/ACCESS.2021.3059746

Suppression of Back-Reflection From the End Face of Si_3N_4 Waveguide Resonator

CHANGKUN FENG, DANNI LIU, PEIREN NI, HUI LI, (Member, IEEE), AND LISHUANG FENG

Key Laboratory of Micro-nano Measurement, Manipulation and Physics (Ministry of Education), Beihang University, Beijing 100191, China
School of Instrumentation and Optoelectronics Engineering, Beihang University, Beijing 100191, China

Corresponding authors: Lishuang Feng (fenglishuang@buaa.edu.cn) and Hui Li (lihui@buaa.edu.cn)

This work was supported in part by the National Natural Science Foundation of China under Grant 61973019.

ABSTRACT Silicon nitride waveguide (Si_3N_4), is used as the most important sensitive device because of its excellent high-polarizing characteristics. It has the potential to build the miniaturized, high-precision resonant integrated optical gyroscope (RIOG) in recent years. However, the back-reflection caused by the refractive index difference between the Si_3N_4 waveguide and the pigtail fiber has a non-negligible impact on the accuracy of the gyroscope. In this paper, we propose a method to suppress the back-reflection of the end face of the Si_3N_4 waveguide resonator. We use the *Fimmprop* module of the simulation software *Photon Design* to simulate the relationship between the back-reflection coefficient of Si_3N_4 waveguide and different tilt angles. The simulation result shows that when the end face of the Si_3N_4 waveguide is oblique cut by 15°, the back-reflection is the minimum, about -67 dB. The back-reflection obtained through the experiments are about -65 dB, consistent with the simulation result. Together, our data suggested that the back-reflection noise of the Si_3N_4 can be suppressed by the oblique cutting of the end face by 15°. The conclusion can lay a foundation for improving the performance of RIOG based on Si_3N_4 waveguide resonator.

INDEX TERMS Back-reflection, integrated optical gyroscopes, oblique cut, silicon nitride waveguides.

I. INTRODUCTION

The optical gyroscope is a type of optical sensor used to measure the rotational angular velocity based on the optical Sagnac effect [1]–[6]. Compared with the current mature interferometric optical gyroscope and laser gyroscope [7], the resonant integrated optical gyroscope (RIOG) has the advantages of high theoretical accuracy and easy integration, and has become a representative of a new generation of sensors. And the RIOG based on the waveguide resonator outrank the others in cost, volume, weight and power consumption. The optical waveguide resonator uses the resonance effect to achieve hundreds or even thousands of times the equivalent optical path in a short geometric optical path, which greatly enhances the detection sensitivity of the Sagnac effect. Thus, high sensitivity detection of angular velocity can be realized in a small size [8], [9].

Despite the current research passion on the RIOG based on the silica waveguide resonator, there are a few defects of the system. The core layer of the silica waveguide is designed to have an approximately square structure with low polarization sensitivity, but it could also introduce polarization noise [10].

The associate editor coordinating the review of this manuscript and approving it for publication was Weidong Zhou.

And the polarization performance of the waveguide resonator is related to temperature. When the ambient temperature changes, the birefringence difference of the waveguide fluctuates. The fluctuation supports the simultaneous transmission of two polarization states in the waveguide resonator, and cause the energy coupling between the primary (i.e. TE mode) and secondary polarization states (i.e. TM mode) to rapidly deteriorate the performance of the gyroscope. This is the most important factor affecting long-term stability of RIOG and limits its performance. One of the most effective methods to solve the problem is to introduce high polarization-dependent loss to make the loss of the TM mode as large as possible. When the external environment changes, the waveguide resonator can always work in high polarization mode, thereby reducing the influence of polarization errors on the performance of the RIOG. Si_3N_4 waveguide is expected to be an effective way to solve this problem. It has ultra-low loss and high-aspect-ratio in the core layer [11]–[14]. In the TM polarization direction, the light confinement of the waveguide core is weak, so a slight bend could produce a huge transmission loss. But the waveguide core is capable to confine light in the TE polarization direction. Since the surface roughness of the waveguide core is very low, theoretically the Si_3N_4waveguide can achieve lower transmission loss than the

silica waveguide. Therefore, Si_3N_4 waveguide could produce waveguide resonators with high fineness and polarization.

However, the back-reflection noise is the most important factor affecting the short-term performance of the RIOG [15], limits the short-term performance of the RIOG, so it cannot meet the requirements of current high-performance tactical applications [16], [17]. The back-reflection discussed occurs in the medium interface outside the waveguide resonator, such as the end faces of waveguides. The interference between the signal and the back-reflection can cause zero-bias fluctuation [7]. It is particularly important to evaluate and eliminate the back-reflection noise when designing a RIOG with high performance [18].

Many research has been done on the influence of the back-reflection outside the waveguide resonator on the RIOG. Takahashi *et al*, for the first time, theoretically and experimentally analyzed the effects of out-cavity back-reflections on the drift characteristics of the resonant fiber optical gyroscope (RFOG) [19]. They proved that the back-reflection signal outside the resonator deteriorates the asymmetry of the resonant curve and thus results in the drift of the RFOG output signal. Feng *et al.* proposed a hybrid phase-modulation technology (HPT) to suppress back-reflection noise, and proved the effectiveness of this technology [5]. The group also proposed the use of phase difference traversal (PDT) method to reduce the back-reflection noise in the hybrid RIOG [7]. With the phase difference between the CW and CCW input light-waves forced to traverse the interval [0], $[2\pi]$ repeatedly and rapidly, the fluctuation will be low-pass filtered. Therefore, the back-reflection noise of waveguide end face can be effectively suppressed. However, there are few reports on RIOG based on Si_3N_4 waveguide resonators, and no studies are on methods to suppress the back-reflection noise caused by the end faces of Si_3N_4 from the Si_3N_4 waveguide resonator itself.

In this paper, the end face of the Si_3N_4 waveguide resonator is oblique cut to suppress the back-reflection noise caused by the waveguide end faces. We model and analyze the influence of back-reflection for gyroscope bias stability. And we use the *Fimmprop* module of the simulation software *Photon Design* to simulate the relationship between the back-reflection coefficient and the different tilt angles with different treatment methods. The simulation results show that the end face back-reflection able to achieve maximum suppression when the end face of the Si_3N_4 waveguide is oblique cut by 15°, about -67 dB. According to the simulation results, we conduct a comparative experiment. The Si_3N_4 waveguide was obliquely cut or polished by 15°, respectively. The measured minimum back-reflection coefficient is about -65 dB, consistent with the theoretical simulation.

II. THE BACK-REFLECTION IN RIOG

The RIOG uses high coherence narrow linewidth laser as the light source, and its coherence length can reach tens or even hundreds of kilometers. Therefore, any two beams of light with the same direction of propagation and polarization in the optical path can be considered completely coherent. The back-reflection light in RIOG optical path is coherent with the signal light, which will affect the resonance curve of the waveguide resonator.

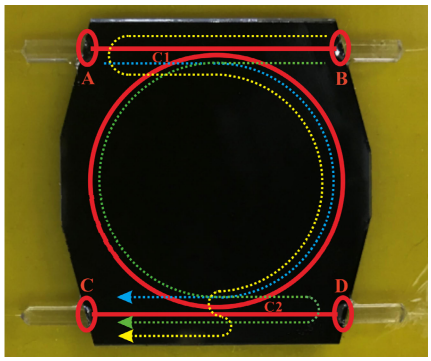

FIGURE 1. Schematic diagram of generating back-reflection noise.

The back-reflection in the optical path of the RIOG based on the Si_3N_4 waveguide resonator mainly comes from the Fresnel back-reflection at the end face of the waveguide resonator and the end face of the optical fiber. At the coupling end face, the effective refractive index of the waveguide mismatches, producing the Fresnel back-reflection phenomenon. The schematic diagram of signal light and back-reflection transmission is shown in Fig. 1. The back-reflection occurs at the coupling points A, B, C and D between the optical fiber and the Si_3N_4 waveguide. For the CW direction, E_A enters the waveguide resonator along the CW direction and outputs from the C port, which is the expected signal light shown in the blue dashed arrow. In the CCW direction, the yellow and green dashed arrows indicate that the incident light has back-reflection at point A and point D, which eventually will be output along the C port. The back-reflection interferes with the signal light, and causes changes in the amplitude of the detection signal. The influence of back-reflection must be restrained to improve the accuracy of RIOG.

The light beams between the reflection points of the light path are reflected back and forth, forming a multi-beam interference effect. Since the higher-order reflection has relatively small influence, only the influence of the primary reflection is considered in this study.

During the transmission of the back-reflection light, it passes through the transmission end, and its electric field amplitude transfer function is:

$$T(\omega) = \sqrt{k_{C1}}\sqrt{k_{C2}}\sqrt{1-\alpha_{C1}}\sqrt{1-\alpha_{C2}}\sqrt{1-\alpha_{L/2}} \cdot \frac{e^{-i\omega\frac{\tau}{2}}}{1-qe^{-i\omega\tau}} \quad (1)$$

The light also passes through the reflection end, with the amplitude transfer function:

$$T'(\omega) = \frac{\sqrt{1-\alpha_{C1}}}{\sqrt{1-k_{C1}}}\left(1-\frac{k_{C1}}{1-qe^{-i\omega\tau}}\right) \quad (2)$$

where $q = \sqrt{1-k_{C1}}\sqrt{1-\alpha_{C1}}\sqrt{1-k_{C2}}\sqrt{1-\alpha_{C2}}\left(1-\alpha_{L/2}\right)$, k_C is the coupling coefficient of the waveguide coupler, α_C is the additional loss of the coupler, α_L is the transmission loss

of the waveguide, and$\tau$is the time for light to travel around a resonator. We assume that the parameters of the two couplers used in the waveguide resonator are the same, so the transfer function is applicable to both couplers. Assuming that the reflectivity of point A and point D is r_A and r_D, the transfer function of the path B→D→C in Fig. 1 is:

$$H(\omega) = T(\omega) \cdot \sqrt{r_D} \cdot T'(\omega) \cdot e^{-i\omega\tau'} \tag{3}$$

where τ' is the transmission time of the beam from the coupling end face of the WRR to the coupler. Similarly, the transfer function of the path B→A→C is:

$$H'(\omega) = T'(\omega) \cdot \sqrt{r_A} \cdot T(\omega) \cdot e^{-i\omega\tau''} \tag{4}$$

The incident light can be treated as a series of light superposition of equally spaced frequency components after phase modulation. If the same modulation frequency is used in the CW and CCW directions, the electric field amplitude entering the phase modulator is E_0, which is expanded according to the Bessel formula with the high-order frequency components ignored. In Fig. 1, the emitted electric field at end C along the path B→D→C is:

$$E_{BDC} = E_0 \left\{ \sum_{n=-\infty}^{\infty} \left[i^n J_n(\beta) e^{i(\omega t + n\Omega t)} \right] \right\} \cdot H(\omega + n\Omega) \tag{5}$$

Similarly, the output electric field at end C along the B→A→C and A→C path are:

$$E_{BAC} = E_0 \left\{ \sum_{n=-\infty}^{\infty} \left[i^n J_n(\beta) e^{i(\omega t + n\Omega t)} \right] \right\} \cdot H'(\omega + n\Omega) \tag{6}$$

$$E_{AC} = E_0 \left\{ \sum_{n=-\infty}^{\infty} \left[i^n J_n(\beta) e^{i(\omega t + n\Omega t)} \right] \right\} \cdot T(\omega + n\Omega) \tag{7}$$

Finally, the total electric field output at the C terminal is:

$$\begin{aligned} E_C &= E_{AC} + E_{BDC} + E_{BAC} \\ &= E_0 \left\{ \sum_{n=-\infty}^{\infty} \left[i^n J_n(\beta) e^{i(\omega t + n\Omega t)} \right] \right\} \\ &\quad \cdot \begin{bmatrix} T(\omega + n\Omega) + H(\omega + n\Omega) \\ + H'(\omega + n\Omega) \end{bmatrix} \end{aligned} \tag{8}$$

Then the output optical *power* P_{out} can be expressed as:

$$\begin{aligned} P_{out} &= E_C \cdot E_C^* \\ &= 2 \cdot E_o^2 \left(\sum_{m=-\infty}^{\infty} J_{m+1}(\beta) J_m(\beta) \right) \\ &\quad \cdot \left[\begin{array}{l} -\sin(\Omega t) \cdot Re \left[\begin{pmatrix} T(\omega + (m+1)\Omega) \\ + H(\omega + (m+1)\Omega) \\ + H'(\omega + (m+1)\Omega) \end{pmatrix} \cdot \begin{pmatrix} T(\omega + (m+1)\Omega) \\ + H(\omega + (m+1)\Omega) \\ + H'(\omega + (m+1)\Omega) \end{pmatrix}^* \right] \\ -\cos(\Omega t) \cdot Im \left[\begin{pmatrix} T(\omega + (m+1)\Omega) \\ + H(\omega + (m+1)\Omega) \\ + H'(\omega + (m+1)\Omega) \end{pmatrix} \cdot \begin{pmatrix} T(\omega + (m+1)\Omega) \\ + H(\omega + (m+1)\Omega) \\ + H'(\omega + (m+1)\Omega) \end{pmatrix}^* \right] \end{array} \right] \end{aligned} \tag{9}$$

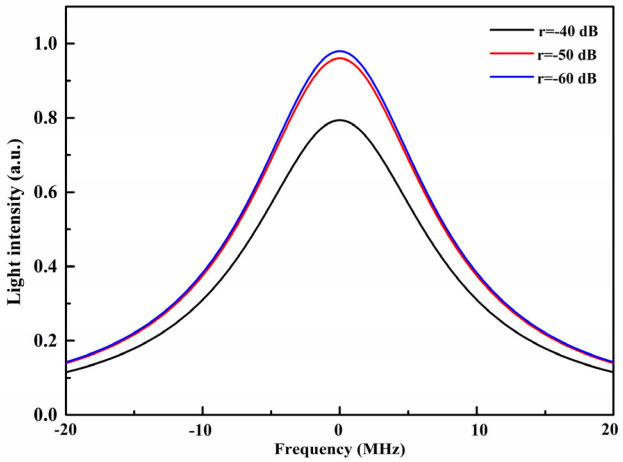

FIGURE 2. The influence of back-reflection noise on the resonance peak.

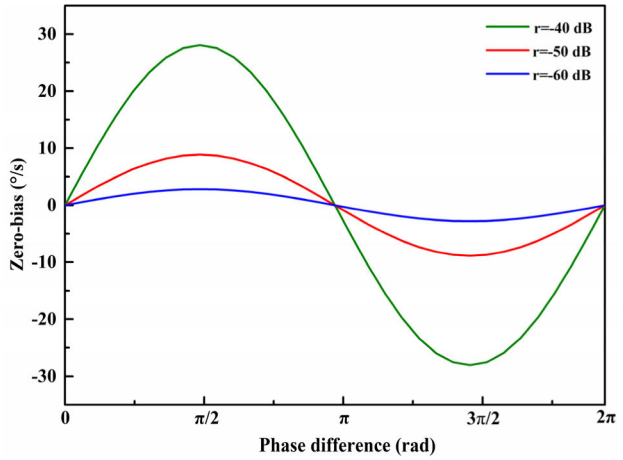

FIGURE 3. The influence of back-reflection noise on the zero-bias.

The above function established thehe above function established the relationship between back-reflection coefficient and gyroscope output. When the incident light is not phase modulated and the light intensities of CW and CCW are the same, we assume that the output time from each end face reflection point to the coupler is equal. The influence of back-reflection on the resonance peak is shown in Fig. 2. We can see that back-reflection will change the height of the resonance peak.

The phase difference between the back-reflection light and the signal light at the detection point C also changes with fluctuation in the external environment. Figure. 3 shows the zero bias change corresponding to the change of the resonance point when the back-reflection coefficient is -40 dB, -50 dB and -60 dB, respectively. The trend of changing is close to a sinusoidal curve. The greater the back-reflection noise, the worse the accuracy of the corresponding RIOG. If the RIOG is working in a large temperature range, even a back-reflection light with a small reflectivity will seriously deteriorate the bias stability of the device. Hence, suppressing the back-reflection light is of great significance to the study of high-precision RIOG.

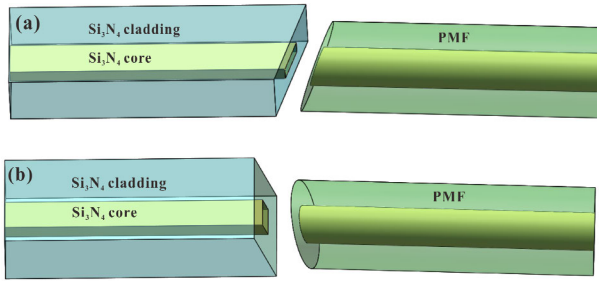

FIGURE 4. Schematic diagram of oblique cutting and oblique polishing of Si_3N_4 waveguide end face, (a) oblique cutting, (b) oblique polishing.

III. BACK-REFLECTION SUPPRESSION METHOD

In order to suppress the back-reflection without weakening the transmission coupling efficiency [20], the end face of the waveguide is usually oblique cut or oblique polished at a suitable angle and aligned according to the refractive index. But for the different waveguide materials, the treatment of the end face is different. Figure 4 are the schematic diagram of Si_3N_4 waveguide end face under oblique cutting (a) and oblique polishing (b). And most of the back-reflected light from the end face leaks into the substrate and cannot form a guided mode to continue transmission in the waveguide.

When the polarization maintaining fiber (PMF) is coupled with the end face of the waveguide, the angle of oblique cutting or oblique polishing is determined according to the following equation:

$$n_{PMF} \sin\alpha = n_{Si_3N_4} \sin\theta \tag{10}$$

where n_{PMF} and $n_{Si_3N_4}$ are the effective refractive indexes of the PMF and the Si_3N_4 waveguide, respectively. α and θ are the tilt angles of the PMF and Si_3N_4 waveguide end faces, respectively. And n_{PMF} is 1.454, $n_{Si_3N_4}$ is 1.447. The difference between the two is very small, so, when the end faces are coupled, the same tilt angle is used. In addition, the selection of the tilt angle is particularly important. We used the *Fimmprop* module of the simulation software *Photon Design* to simulate the back-reflection coefficient under different tilt angles.

Figure 5 shows the simulation results of the end face back-reflection coefficient of the Si_3N_4 waveguide at different tilt angles, when the end face is processed by oblique cutting or oblique polishing. With the oblique polishing method is used, the minimum back-reflection coefficient is about -55 dB. When the end face of the Si_3N_4 waveguide is obliquely cut, the back-reflection coefficient is generally smaller and the minimum coefficient about -67 dB, is reached at the tilt angle of 15°. Through simulation, we see that the back-reflection noise can be effectively reduced when the end face of the Si_3N_4 waveguide is processed by the oblique cutting method. The method is promising to reduce the influence of the back-reflection noise and improve the performance of RIOG.

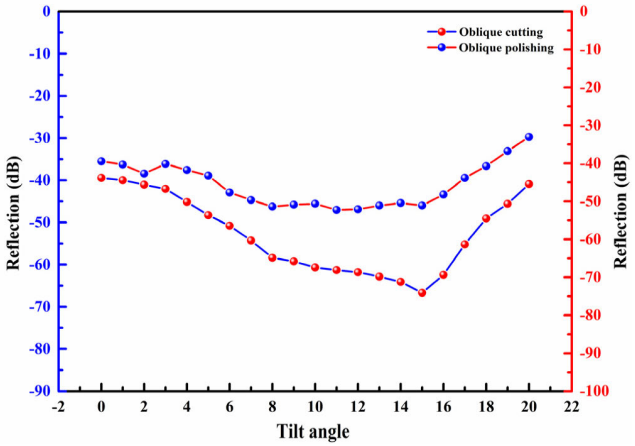

FIGURE 5. The back-reflection coefficient at different tilt angles.

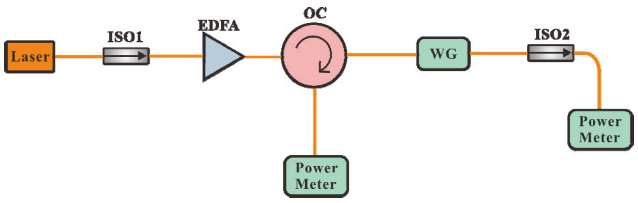

FIGURE 6. The back-reflection coefficient of Si_3N_4 waveguide test system device. ISO: isolator, EDFA: erbium doped optical fiber amplifier, OC: optical circulator, WG: waveguide.

IV. EXPERIMENTAL RESULTS

We further verified the simulation results by experiments. Figure 6 shows the test device diagram for measuring the end face back-reflection coefficient of the Si_3N_4 waveguide. It is mainly composed of a laser, an erbium doped optical fiber amplifier (EDFA), two optical isolators (ISO), an optical circulator (OC), the Si_3N_4 waveguide and optical power meter.

Laser is amplified by the EDFA and input to the OC through ISO1, which is used to prevent the reflected light from affecting the stability of the laser. Then the light enters the waveguide through the OC. The light wave is transmitted in the waveguide, and output through the ISO2. An optical power meter records the output light power value. The reflected light is output through the reflecting end of the OC (i.e. the back-reflected light), with its power value is recorded being measured by second optical power meter. Assuming the output power of the laser is P_1 and the reflected light is P_2, the back-reflection coefficient of the waveguide end face can be calculated from the equation $-10\log(P_2/P_1)$.

Three Si_3N_4 straight waveguides with different treatment methods were used in the experiment. i) The end face of the waveguide was directly coupled to the PMF at 0°. ii) The end face of the Si_3N_4 was obliquely polished at 15°. iii) The end face was obliquely cut at 15°. Six replicates were conducted for each method. And the six groups of experiments were conducted for each method.

For each condition, 500 groups of data were collected and the averaged value was taken as the end face back-reflection noise value. Figure 7 shows the back-reflection coefficient

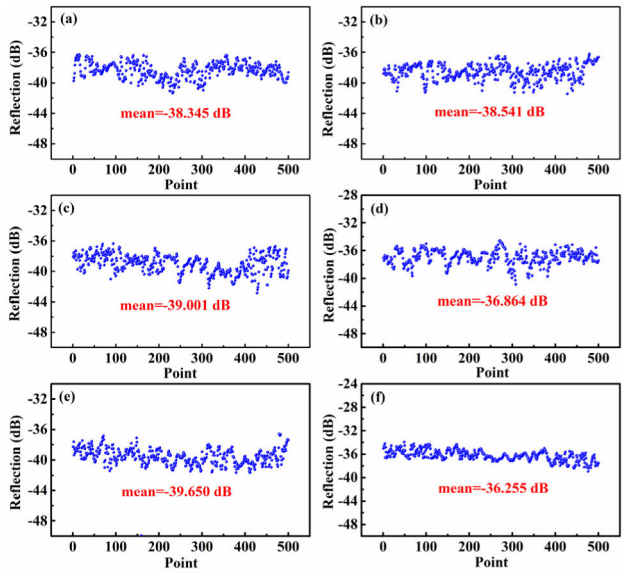

FIGURE 7. The back-reflection coefficient of the end face of the Si_3N_4 waveguide when the end face is directly coupled.

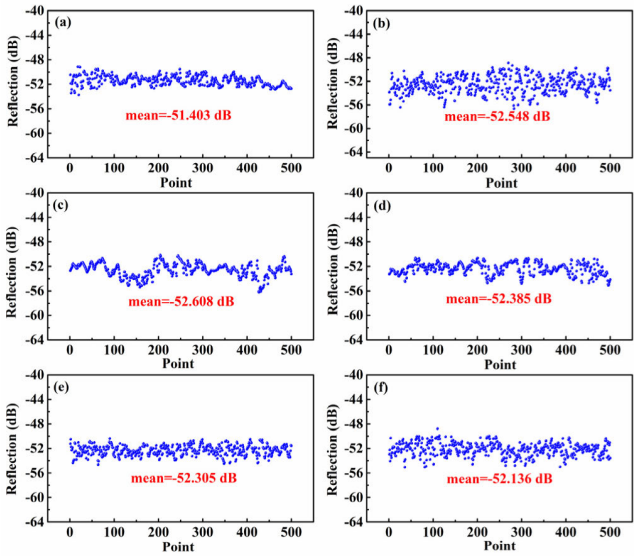

FIGURE 8. The back-reflection coefficient of the Si_3N_4 waveguide when the end face is oblique polished by 15°.

values of the six straight waveguides when they were directly coupled with the PMF at 0°. The back-reflection coefficients are -38.345 dB, -38.541 dB, -39.001 dB, -36.864 dB, -39.650 dB and -36.255 dB from (a) to (f). The test result of oblique polishing at 15° is shown in Fig. 8 and the back-reflection coefficients are -51.403 dB, -52.548 dB, -52.608 dB, -52.385 dB, -52.305 dB and -52.136 dB, respectively.

When the end face of the Si_3N_4 waveguide is oblique cut by 15°, the back-reflection coefficients are -65.134 dB, -62.974 dB, -65.835 dB, -65.845 dB, -63.417 dB and -63.612 dB, respectively. The test result is shown in Fig. 9(a)-(f). Through the above comparison experiments, we found that the maximum suppression of the end face back-reflection can be achieved by obliquely cutting the end

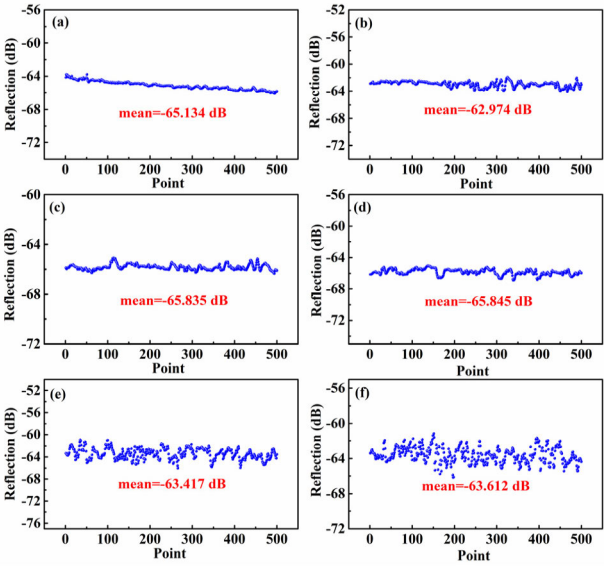

FIGURE 9. The back-reflection coefficient of the Si_3N_4 waveguide when the end face is when the end is face oblique cut by 15°.

face at 15° for the Si_3N_4 waveguide. The experimental results are consistent with the simulation.

V. DISCUSSIONS

As in all RIOG setups, the back-reflection noise is one of the most important factors affecting its performance, hindering the construction of high-precision RIOGs. Multiple methods for suppressing the back-reflection noise were proposed, such as carrier-suppression with double phase modulation technique (DPMT) [21], technology of HPT and PDT [5], [6], and a three-laser scheme in which two laser frequencies are locked onto third laser [22]. These methods can achieve exceptionally good carrier suppression, so the RIOG could work under non-optimal phase modulation amplitudes and instable ambient temperatures [19]. However, the drift caused by the multi-reflections between the two entrances of the resonator cannot be suppressed by the carrier-suppressed PMT described above [21].

At present, we are the first to study the back-reflection suppression at the end face of a Si_3N_4 waveguide resonator. We found, through simulations and experiments, a 15° oblique cutting at the end face of a Si_3N_4 waveguide can effectively suppress the back-reflection. This method only processes the waveguide and is easy to implement. However, the method has higher requirements on the cutting and the coupling process. If there is an angular deviation during the cutting and coupling alignment, the waveguide resonator will have residual back-reflection. And in actual operations, the angle deviations often exist. The entire RIOG system includes optical components such as lithium niobate phase modulators, the coupling between PMFs will also cause back-reflection noise, which will affect the performance of the gyroscope. Therefore, the above carrier suppression methods are also applicable to RIOG based on Si_3N_4 waveguides. In the next step, we will combine the two methods to

effectively eliminate the residual back-reflection caused by process errors, looking to obtaining a Si_3N_4 waveguide based RIOG with higher precision.

VI. CONCLUSION

The Si_3N_4 waveguides have excellent high polarization, so the RIOG based on Si_3N_4 waveguide resonators have received more attention currently. However, the back-reflection caused by the end faces of Si_3N_4 waveguides seriously affect the performance of RIOG and becomes an immediate issue to be solved. but the back-reflection caused by the end faces of Si_3N_4 waveguides seriously affect the performance of RIOG. In this paper, we proposed that oblique cutting and oblique polishing can successfully suppress the back-reflection noise of Si_3N_4 waveguide resonator. Both the theoretical simulations and the on-site experiments showed that the back-reflection noise is minimum when the end face of the Si_3N_4 waveguide was obliquely cut by 15°. Under this condition, the back-reflection coefficient measured by the theoretical simulation and the experiment are about -67 dB and -65 dB, respectively. This is better than the back-reflection coefficient of -52 dB with oblique polishing by 15°. The experimental and simulation results are highly consistent. This finding lays a foundation for improving the performance of RIOG based on Si_3N_4 waveguide resonators.

REFERENCES

[1] N. Barbour and G. Schmidt, "Inertial sensor technology trends," *IEEE Sensors J.*, vol. 1, no. 4, pp. 332–339, Dec. 2001.
[2] Y. Yang, D. Chen, W. Jin, W. Quan, F. Liu, and J. Fang, "Investigation on rotation response of spin-exchange relaxation-free atomic spin gyroscope," *IEEE Access*, vol. 7, pp. 148176–148182 , 2019.
[3] C. Ciminelli, F. Dell'Olio, C. E. Campanella, and M. N. Aremenise, "Photonic technologies for angular velocity sensing," *Adv. Opt. Photon.*, vol. 2, no. 3, pp. 370–404, Jun. 2010.
[4] C. Ciminelli, C. E. Campanella, and M. N. Armenise, "Optimized design of integrated optical angular velocity sensors based on a passive ring resonator," *J. Lightw. Technol.*, vol. 27, no. 14, pp. 2658–2666, Jul. 2009.
[5] L. S. Feng, M. Lei, H. L. Liu, Y. Z. Zhi, and J. J. Wang, "Suppression of back-reflection noise in a resonator integrated optic gyro by hybrid phase-modulation technology," *Appl. Opt.*, vol. 2013, vol. 52, no. 8, pp. 1668–1675, Oct. 2013.
[6] J. J. Wang, L. S. Feng, Q. W. Wang, H. C. Jiao, and X. Wang, "Suppression of back-reflection error in resonator integrated optic gyro by the phase difference traversal method," *Opt. Lett.*, vol. 41, no. 7, pp. 1586–1589, Mar. 2016.
[7] Y. Tao, S. Li, and S. Liu, "Analysis and improvement of frequency stabilization characteristics of a total reflection prism laser gyro," *IEEE Access*, vol. 6, pp. 69185–69194, 2018.
[8] C. Monovoukas, A. K. Swiecki, and F. Maseeh, "Integrated optical gyroscopes offering low cost, small size and vibration immunity," *Proc. SPIE*, vol. 3936, pp. 293–300, Jan. 2000.
[9] F. Dell'Olio, T. Tatoli, C. Ciminelli, and M. N. Armenise, "Recent advances in miniaturized optical gyroscopes," *J. Eur. Opt. Society, Rapid Publications*, vol. 9, p. 14013, Mar. 2014.
[10] L. S. Feng, J. J. Wang, Y. Z. Zhi, Y. C. Tang, Q. W. Wang, H. Li, and W. Wang, "Transmissive resonator optic gyro based on silica waveguide ring resonator," *Opt. Exp.*, vol. 22, no. 22, pp. 27565–27575, Oct. 2014.
[11] J. F. Bauters, M. J. R. Heck, D. John, D. X. Dai, and E. B. John, "Ultra-low-loss high-aspect-ratio Si_3N_4 waveguides," *Opt. Exp.*, vol. 19, no. 4, pp. 3163–3174, Feb. 2011.
[12] M. C. Tien, J. F. Bauters, M. J. R. Heck, D. T. Spencer, and J. E. Bowers, "Ultra-high quality factor planar Si_3N_4 ring resonators on SI substrates," *Opt. Exp.*, vol. 19, no. 14, pp. 13551–13556, Jun. 2011.
[13] J. Guo, M. J. Shaw, G. A. Vawter, P. Esherick, G. R. Hadley, and C. T. Sullivan, "High-Q integrated on-chip micro-ring resonator," in *Proc. 17th Annu. Meeting IEEE Lasers Electro-Optics Soc. LEOS*, Dec. 2004, pp. 745–746.
[14] S. Srinivasan, R. Moreira, D. Blumenthal, and J. E. Bowers, "Design of integrated hybrid silicon waveguide optical gyroscope," *Opt. Exp.*, vol. 22, no. 21, pp. 24988–24993, 2014.
[15] H. Ma, J. Zhang, L. Wang, and Z. Jin, "Development and evaluation of optical passive resonant gyroscopes," *J. Lightw. Technol.*, vol. 35, no. 16, pp. 3546–3554, Aug. 15, 2017.
[16] C. Ciminelli, F. Dell'Olio, and M. N. Armenise, "High-Q spiral resonator for optical gyroscope applications: Numerical and experimental investigation," *IEEE Photon. J.*, vol. 4, no. 5, pp. 1844–1854, Oct. 2012.
[17] K. Iwatsuki, K. Hotate, and M. Higashiguchi, "Backscattering in an optical passive ring-resonator gyro: Experiment," *Appl. Opt.*, vol. 25, no. 23, pp. 4448–4451, Dec. 1986.
[18] X. Zhang and K. Zhou, "Analysis on two-reflection-dots model outside resonator of R-MOG," *Chin. J. Sens. Actuators*, vol. 22, pp. 811–815, Jun. 2009.
[19] M. Takahashi, S. Tai, and K. Kyuma, "Effect of reflections on the drift characteristics of a fiber-optic passive ring-resonator gyroscope," *J. Lightw. Technol.*, vol. 8, no. 5, pp. 811–816, May 1990.
[20] H. J. Arditty, H. J. Shaw, M. Chodorow, and R. K. Kompfner, "Re-entrant fiber-optic approach to rotation sensing," *Proc. SPIE*, vol. 157, pp. 138–148, Dec. 1978.
[21] H. Mao, H. L. Ma, and Z. H. Jin, "Polarization maintaining silica waveguide resonator optic gyro using double phase modulation technique," *Opt. Exp.*, vol. 19, no. 5, pp. 4632–4643, Feb. 2011.
[22] J. Wu, M. Smiciklas, L. K. Strandjord, T. Qiu, W. Ho, and G. A. Sanders, "Resonator fiber optic gyro with high backscatter-error suppression using two independent phase-locked lasers," *Proc. SPIE*, vol. 9634, Oct. 2015, Art. no. 96341O.

CHANGKUN FENG received the M.S. degree from the School of Taiyuan University of Technology of China. He is currently pursuing the Ph.D. degree with the School of Instrumentation and Optoelectronic Engineering, Beihang University. His research interest includes resonant integrated optical gyro based on silicon nitride resonator cavity.

DANNI LIU received the B.S. degree from the School of Instrument and Electrics, North University of China. She is currently pursuing the Ph.D. degree with the School of Instrumentation and Optoelectronic Engineering, Beihang University. Her research interest includes integrated optical gyros.

PEIREN NI received the B.S. degree from the School of Instrumentation and Optoelectronic Engineering, Beihang University, where he is currently pursuing the M.S. degree. His research interest includes resonant integrated optical gyro.

HUI LI (Member, IEEE) received the Ph.D. degree from the School of Instrumentation and Optoelectronic Engineering, Beihang University, China, in 2009. She is currently an Associate Professor with the School of Instrumentation and Optoelectronic Engineering, Beihang University. She has authored or coauthored over 40 papers in refereed journals and conference proceedings. Her current research interests include optical sensors, integrated optics, signal processing, time-delay systems, and robust control.

LISHUANG FENG received the Ph.D. degree from the Saint Petersburg Institute of Fine Mechanics and Optics, Russia, in 1996. From 1997 to 2001, she was an Associate Professor with the School of Photoelectronic Information and Communication Engineering, Beijing Information Science and Technology University. She joined the School of Instrumentation and Optoelectronic Engineering, Beihang University, in 2001, where she is currently a Professor. She has authored or coauthored over 100 papers in refereed journals and conference proceedings. Her research interests include integrated optics and MOEMS systems, advanced optical sensors, and optoelectronics devices.